NASA

Technical Memorandum **80659**

The Cosmic X-Ray Background

E. A. Boldt

March 1980

National Aeronautics and
Space Administration

Goddard Space Flight Center
Greenbelt, Maryland 20771

THE COSMIC X-RAY BACKGROUND

An Invited Lecture at the 155th Meeting
American Astronomical Society
San Francisco, California

January 15, 1980

Elihu Boldt

Laboratory for High Energy Astrophysics
NASA/Goddard Space Flight Center
Greenbelt, Maryland 20771

ABSTRACT

The cosmic X-ray experiment carried out with the A2 Instrument* on HEAO-1 was especially developed to make systematics-free measurements of the extragalactic X-ray sky and has yielded the broadband spectral characteristics for two extreme aspects of this radiation. For the apparently isotropic radiation of cosmological origin that dominates the extragalactic X-ray flux (> 3 keV), the spectrum over the energy band of maximum intensity is remarkably well described by a thermal model with a temperature of a half-billion degrees (i.e. kT $\approx$ 40 keV). At the other extreme, broadband observations of individual extragalactic X-ray sources with HEAO-1 are restricted to objects within the present epoch. These X-ray sources include a large sample of active galaxies studied in some detail over a broad bandwidth for the first time. While the non-thermal hard spectral components associated with unevolved X-ray emitting active galaxies could account for most of the gamma-ray background, the contribution of such sources to the X-ray background must be relatively small. In contrast, the "deep-space" sources detected in soft X-rays with the Einstein Observatory (HEAO-2) telescope probably represent a major portion of the extragalactic soft X-ray (< 3 keV) background, the characteristics of which are not yet firmly established. The contribution of these very remote sources to the well determined hard X-ray background, however, depends most critically on

*The HEAO-1 A2 experiment is a collaborative effort led by E. Boldt of Goddard Space Flight Center and G. Garmire of the California Institute of Technology.

their broadband spectra, which are inaccessible with current experiments. If their spectra are similar to those measured for nearby active galaxies, then their contribution to the background can not be large enough to significantly affect the overall thermal type spectrum observed. In such a situation, we have to consider new sources of emission peculiar to an earlier epoch and/or diffuse intergalactic emission. Small deviations from isotropy in the cosmic X-ray background are being studied and the status of results is presented in terms of the geometries associated with the galaxy, the local supercluster and the microwave background.

Our view of the X-ray sky is very different in the soft and hard X-ray bands. For photon energies less than 1 keV or so the Einstein Observatory (HEAO-2) is informing us that stars of every type are X-ray sources. Yet, the surface brightness maps constructed from the all-sky surveys carried out with the broad-band A2 instrument on HEAO-1 show that by far most of the soft X-ray flux is due to large-scale background features associated with our galaxy. This all-sky experiment, especially developed for broad-band studies of the X-ray background (Boldt et al. 1979a; Rothschild et al. 1979), is a collaboration between our group at Goddard and several investigators here in California associated with Gordon Garmire, who will report elsewhere on soft X-ray maps of the entire sky. A particularly interesting large-scale feature in soft X-rays recently discovered with this all-sky survey is called the "X-ray Superbubble in Cygnus", as discussed in this meeting by Cash (1979).

Above a few keV, the situation changes drastically in that most of the flux is associated with an extragalactic background and that any galactic effects away from the galactic plane become a relatively minor perturbation (see Appendix A). This situation of obtaining such an unobscured view of the composite emission of the universe is practically unique in astronomy, the only other example that I know of being the microwave background. This composite extragalactic flux (or "cosmic background") of hard X-rays is the topic of this lecture.

Figure 1 gives an overall view of the sky in hard X-rays; this is an all-sky map of surface brightness, with all sources included, and was constructed by DeAnn Iwan from the 2-60 keV all-sky data base of our A2 experiment. Since the map is in galactic coordinates, the equator and center of the galaxy are quite evident. The data are from High Energy Detector (HED) #1, where the dual fields of view are $6^0 \times 3^0$ and $3^0 \times 3^0$. The counts recorded were simply assigned to $3^0 \times 3^0$ pixels. The resulting intensities for these pixels are color coded. Those intensities within 3% of a constant background are blue. Intensities lower than this are shown as

black, higher are shown as red. Within each color code, the lines per pixel provide a vernier on the numerical intensity. This particular map saturates at a surface brightness about 40% above that of the diffuse background. In terms of source intensity it is equivalent to the brightest isolated galaxy, which is Cen A. A few clusters of galaxies exceed this saturation limit; many galactic sources do, of course. For the present discussion, the main thing to notice is that most of this map is blue, indicating that the cosmic X-ray background is a well-defined dominant aspect of the sky.

The spectrum of the cosmic X-ray background is remarkably simple. Figure 2 shows the results of a spectral analysis by Marshall et al. (1980) of the X-ray flux as observed at high galactic latitudes away from resolved hard X-ray sources. What is plotted here is the ratio (R) of the observed flux to that predicted for three different thermal models as a function of photon energy. There are many different symbols used for these plots, corresponding to the fact that the A2 instrument examined this flux in many different ways in order to minimize any systematic bias. What we see here is that the correct temperature is about a half-billion degrees (i.e. kT $\approx$ 40 keV). From about 3 to 20 keV the statistical error bars are smaller than the size of the symbols used and deviations from unity for the best fit are generally less than $\sim$1%. In fact, given the large bandwidth, high statistical significance, and goodness of fit involved, I conclude that this is one of the best known spectra in X-ray astronomy, certainly better known than that of any single extragalactic source. It's important to remember, though, that our knowledge of the extragalactic background in soft X-rays and gamma-rays is still relatively imprecise.

Now that we know the properties of the integral extragalactic flux of hard X-rays we are ready to examine models. For evaluating the contribution of discrete sources we need source counts up to high redshifts and broad-band spectra for several sources representing all classes of emitters. Until HEAO-1 and HEAO-2 such information was essentially absent. Now, HEAO-2 is beginning to give us the source counts we need, but in the soft X-ray band. HEAO-1 gives us source spectra in the hard X-ray band needed, but only for objects in the present epoch. With

the obvious and crucial observational gap still with us, there is room for discussion and we proceed to examine what we know and what we think we know.

In searching for sources that are thermal we must first consider clusters of galaxies. The Perseus cluster is the brightest extragalactic source and Figure 3 shows its spectrum in terms of photon flux versus photon energy. This is the characteristic spectrum of a plasma at a temperature of about 80 million degrees, quite typical of known clusters. It shows the well resolved K lines of collisionally excited helium type iron ions at 6.7 keV and at 7.9 keV and unresolved lines of Si, S, Ca and Ar between $\sim$ 2 and 4 keV. The luminosity of $\sim 10^{45}$ ergs s^{-1} is among the highest for clusters. As far as their contribution to the background, the observed spectrum of the background itself provides us with two important constraints. First of all, since the temperature of the background is an order of magnitude higher than that of the 30 or so clusters examined, their contribution to the background must be restricted to the lower energy end (unless there is an unexpected severe evolution in temperature). Secondly, since there is no detectable discontinuity in the background spectrum above and below $\sim$ 7 keV, the contribution of iron line emission is definitely limited; this implies that the contribution of clusters at $\sim$ 7 keV is at most a few percent. The all-sky survey provided by HEAO-1 has also been used to estimate a luminosity function for clusters. In order to work with a complete sample, McKee et al. (1980) have recently used the Abell clusters of distance class up through 4 in the Leir-van den Bergh catalog (1977) to search for X-ray sources. This most recent work yields that the contribution of clusters is probably only about 4% at the lowest energies of the measured background.

Isolated galaxies are also X-ray sources; our own galaxy has a luminosity of a few x 10^{39} erg s^{-1}. Worrall et al. (1979) have used the all-sky data base of the A2 experiment on HEAO-1 to search for the average hard X-ray emission from 78 well isolated galaxies within 20 Mpc and conclude that our galaxy is not underluminous in X-rays relative to other normal galaxies and that, ignoring possible evolutionary effects, their contribution to the background would be less than one percent.

Some BL Lac type objects exhibit X-ray luminosities comparable to clusters and even higher. We now have broad-band spectra for five of them from HEAO-1. Figure 4 shows one such spectrum (Riegler, Agrawal and Mushotzky 1979). Unlike the spectra for typical clusters which are relatively flat at low energies and then fall off above a few keV, this one is steep at the lowest energies and flattens above a few keV. A typical BL Lac type spectrum is hard to define; sometimes there are two components as in this case and sometimes only the soft component is present. This sort of variation holds from one source to another and also for a given source from one time of observation to another. In any event, their spectra seem never to be similar to that of the X-ray background. Since sources such as these might be closely related to quasars, however, one of the things we should learn from these spectra is how we could be misled in extrapolating HEAO-2 soft X-ray flux measurements to the hard X-ray region of the spectrum.

Apart from BL Lac type objects and possibly quasars, where our spectral knowledge is still meagre, active galaxies exhibit X-ray spectra that are quite uniform. First of all we consider the spectrum of the brightest X-ray galaxy, Centaurus A; this is shown in Figure 5. Cen A is bright mainly because it is relatively nearby; although its X-ray luminosity is about a thousand times that of our galaxy, it is much less luminous than most active galaxies. The spectrum is clearly non-thermal. Below a few keV it shows the pronounced effect of absorption by a large amount of matter. This source has been measured at higher energies than shown in Figure 5 with the A4 instrument on HEAO-1; Baity (1980, private communication) indicates that this power-law spectrum of photon number index 1.6 - 1.7 extends to a few hundred keV and that Cen A is still detectable out to about an MeV.

In addition to the spectrum for Cen A the A2 experiment has already provided us with broad-band spectra for 12 Seyfert-I galaxies, 4 narrow emission line galaxies, 3 N galaxies and 2 quasars out of a total of over 50 isolated galaxies clearly detected in hard X-rays. Five spectra representative of the sample of Seyferts are shown in Figure 6 (Mushotzky et al. 1980). The Seyfert-I galaxies represented here range in luminosity from a few times that of Cen A for NGC 6814 to about a hundred times that of Cen A for MCG 8-11-11. Except for the lowest luminosity galaxy, none of these show anything close to the pronounced absorption exhibited by Cen A. Since the brightest X-ray Seyfert (NGC 4151) shows absorption comparable to Cen A, this initial sample of two gave us the impression that all X-ray spectra from active galaxies would exhibit this effect. In fact, our HEAO data now indicate that only the very lowest luminosity Seyferts, such as NGC4151, share this feature. As far as we can tell, at energies above 3 keV or so, most of the X-ray emitting active galaxies have simple power-law spectra with photon number indices that are typically in the vicinity of 1.6 - 1.7.

Excluding BL Lac type objects, a histogram of X-ray spectral indices for active galaxies (see Table 3) obtained with the A2 instrument is shown in Figure 7. This histogram of spectral index values is presented here in terms of the energy index α, offset by one unit from the photon number index Γ discussed before. For the collection of individually measured spectra, "Sample A", α ranges from 0.41 to 0.97. These spectra, for the most part,

were obtained from extended exposures during times when the HEAO-1 spacecraft was pointed. We have also considered sources detected during the normal all-sky scans performed with HEAO-1. In these scans, there were 29 well isolated galaxies detected which are at high galactic latitudes (see Table 3). Considering the composite spectrum for these 29 galaxies, without excluding BL Lac type objects or normal galaxies, Stottlemyer and I find a best-fit $\alpha \approx 0.6$. We call the collection of sources in this composite spectrum "Sample B" and the range of acceptable α's for 90% confidence is here indicated as $(\Delta\alpha)_B$. Samples A and B are clearly consistent. We conclude that one can define an effective typical spectrum for an X-ray emitting galaxy in the present epoch and that, at least for the band 3-50 keV, this spectrum is a power-law of energy index in the vicinity of 0.6 - 0.7.

Can power-law sources such as those just discussed make much of a contribution to the X-ray background? To examine this, we have tried power-law fits to the observed X-ray background spectrum, and two such are shown in Figure 8 (Marshall et al. 1980). As before, we have here plotted the ratio (R) of the observed flux to that predicted by the model considered, as a function of photon energy. We consider two photon number spectral indices. For a thermal spectrum of 40 keV, the Gaunt factor implies that a power-law model of index $\Gamma = 1.4$ should provide a fairly decent fit at the lowest energies and that the ratio plotted here should fall off exponentially at energies that approach kT. This behavior is quite evident in the figure. On the other hand, if we consider a power-law with $\Gamma = 1.7$, more represent-

ative of present epoch active galaxies, we see that the corresponding ratio plotted is unacceptable. Stottlemyer and I have also considered models made up of a thermal spectrum with a contamination corresponding to a power-law of $\Gamma = 1.7$. Referred to the spectral densities at the lowest energy (3 keV), we find that the 99% confidence upper limit to such a contamination is 26%. This limit is relaxed somewhat if a spread of indices comparable to that exhibited in Figure 7 is taken into account. DeZotti (1979, private communication) has done this analysis with the A2 data and finds that he can account for the background if these sources have a rather sharp characteristic spectral break at about 40 - 60 keV. So far, there is no evidence for such a general feature.

Table 1 summarizes what we know about the population of brightest X-ray emitting galaxies in the present epoch. Item I gives some results from the HEAO-1 A2 all-sky survey for a detection threshold where our sample should be complete. For this complete sample, we have restricted ourselves to those 23 sources at high galactic latitude (i.e. $|b| > 20^0$) exceeding the threshold indicated and renormalized for the excluded solid angle.

Item II gives our formal results as far as the local luminosity function is concerned (see Appendix B). In fact the density of over 10^{-4} Mpc^{-3} shown here could be an overestimate due to the local supercluster (deVaucouleurs 1958); Piccinotti (1980, private communication) is looking into this problem further. Estimates of the density of active galaxies within the

Table 1

BRIGHTEST ACTIVE GALAXIES

I - HEAO-1 A2 ALL-SKY SURVEY

$S(3\text{-}50\ \text{keV}) \geq 8.0 \times 10^{-11}$ ERGS $CM^{-2}\ S^{-1}$ *

$N(4\pi) = (37 \pm 8)$ SOURCES

II - LOCAL LUMINOSITY FUNCTION

$n(>L_0) = 1.4 \times 10^{-4}$ MPC^{-3}

$L_0(3\text{-}50\ \text{keV}) \approx 2 \times 10^{42}$ ERGS S^{-1} *

$\langle L \rangle \approx 9 \times 10^{42}$ ERGS S^{-1} *

III - COMPOSITE FLUX OF UNEVOLVED SOURCES ($z < 1$) AT 3 keV *

(PERCENT OF X-RAY BACKGROUND):

(23 ± 9) %

* FOR $\frac{dS}{dE} \propto E^{-0.7}$

present epoch derived from observations outside the X-ray band (Schmidt 1978) are generally lower than our number by at least a factor of 2.

Item III gives the composite flux of active galaxies (for $z \leq 1$) assuming that the luminosity function of item II is correct, that there is no evolution and that the deceleration parameter q_o is zero. Referred to 3 keV, under the assumption of a power-law spectrum of energy index $\alpha = 0.7$, the contribution to the background is about 23%. As already indicated, though, this could be an overestimate due to a possible systematic bias introduced by the local supercluster (see Appendix).

The Einstein Observatory is now providing us with information on X-ray sources at earlier epochs. Deep exposures over small angular regions of the sky give us soft X-ray source counts from remote regions of the universe where the hard X-ray background is likely to originate. These results are summarized in Table 2.

Item I reviews the recently published work by Giacconi et al. (1979). When scaled up to the full sky, their sample corresponds to about a million objects, comparable to conservative estimates of the number of quasars (Wills 1978).

Item II translates the results given in item I into a corresponding composite flux at 3 keV, where we can make contact with the measured background. To do this we need to know the log N-log S relation at intensities at and above the threshold indicated for a complete sample and the typical spectrum over the band from about 1 keV up to about 3 keV. We assume an energy

Table 2

FAINT EXTRAGALACTIC SOURCES

I - HEAO-2 SMALL-FIELD DEEP EXPOSURES:

$S(1\text{-}3\ \text{keV}) \geq 2.6 \times 10^{-14}$ ERGS $CM^{-2} S^{-1}$

$N(4\pi) = (7.9 \pm 3.3) \times 10^{5}$ SOURCES

II - COMPOSITE FLUX OF RESOLVED SOURCES AT 3 keV *

(PERCENT OF X-RAY BACKGROUND):

$(7.1 \pm 2.9) \left(\frac{a}{a-1}\right)$ %

WHERE $a \equiv -(\Delta \text{LOG } N) / (\Delta \text{LOG } S)$

III - COMPOSITE FLUX OF POWER-LAW SOURCES

(PERCENT OF X-RAY BACKGROUND AT 3 keV *):

26 % UPPER LIMIT (SPECTRAL ANALYSIS OF X-RAY BACKGROUND: HEAO-1 A2)

* FOR $\frac{dS}{dE} \propto E^{-0.7}$

spectral index of 0.7 and express our answer in terms of the slope (a) of the log N-log S relation. The percent of the background at 3 keV due to these sources observed with HEAO-2 is then about 7% times a factor that can range between the extremes of unity for high values of (a) to a value of 3 for a = 1.5. In the subsequent discussion we use the maximum value, per Giacconi et al. (1979). If we were to use a $\approx$ 1.9, as discussed at this meeting by Murray (1979) for strongly evolved sources, the coefficient would be $\sim$ 2 instead of 3.

Item III reviews what can be stated about the contribution of assumed power-law sources to the X-ray background based only on an analysis of the spectrum of the background itself. The thing to note here is that the 26% upper limit at 3 keV discussed before is consistent with the percentage expressed in item II, based on HEAO-2 source counts.

From HEAO-1 and HEAO-2 we can now piece together what we think we know about the extragalactic X-ray sky as a whole; this is shown in Figure 9. The surface brightness of the extragalactic X-ray sky is plotted here as a function of photon energy. The curve labelled "total flux" is the best-fit thermal spectrum for the background measured with the A2 instrument on HEAO-1. The power-law "A" represents the composite flux due to sources corresponding to those detected in the deep exposures with HEAO-2, as summarized in Table 2. The power-law "B" represents the composite flux from active galaxies such as those measured with HEAO-1, assuming no evolution. As already indicated, curve "B" might be an overestimate by a factor of 2 or

so, for this particular unevolved component. If we assume that the power-law is strict then curve "B" may be extrapolated to higher energies; this is indicated as a dashed line from 50 to 100 keV. On the basis of what we already know for Cen A, such an extrapolation makes some sense.

Now we are in a position to make contact with the gamma-ray regime. As discussed in this session by Matteson et al. (1979), the A-4 experiment on HEAO-1 has measured the extragalactic background at about 100 keV and somewhat above. Balloon-borne experiments (Kinzer et al. 1978) indicate that the X-ray background spectrum shown (Fig. 9) continues to fall sharply with energy up to 100 keV or so. However, higher energy observations up thru the MeV region, as carried out from various space platforms, suggest that an underlying gamma-ray component emerges above a few hundred keV; this situation is summarized in Figure 10.

Figure 10 exhibits representative data on the extragalactic gamma-ray background over the band 100 keV to 100 MeV. The data points show recent results from the A4 instrument on HEAO-1, for the band from 100 keV to 300 keV, as well as higher energy results obtained by Trombka et al. (1978), based on their Apollo experiments. The dash-dot line above 35 MeV is a power-law fit obtained by Fichtel et al. (1978) for their SAS-2 spark-chamber data. We now compare all these data with an extrapolation of our X-ray results below 50 keV. The dashed line starting at 100 keV is a continuation of power-law "B", as shown previously in Figure 9 and corresponds to our estimate of the contribution of active galaxies to the gamma-ray background. If we add to that a strict

continuation of the best-fit thermal function obtained for the X-ray background, we obtain the solid curve shown in this figure. As exhibited, the resultant extrapolation tracks the data up to a few hundred keV remarkably well, especially if we consider what an unduly severe demand we are making of our thermal fit. It's probably more significant to notice that, when the thermal contribution vanishes, the remaining power-law indicative of active galaxies tends to exceed the gamma-ray background. Ultimately, the gamma-ray background breaks in the MeV region, perhaps reflecting a break in the spectra of active galaxies. We conclude that unevolved active galaxies could readily account for all of the gamma ray background (see also Bignami et al. 1979). Furthermore, the flux level of the gamma-ray background seems to impose a limit to the local X-ray luminosity function of active galaxies, enforcing that it be somewhat smaller than our formal estimate.

Returning to the X-ray regime, our tentative conclusion is that those hard X-ray sources which dominate the gamma-ray regime contribute a relatively small portion of the X-ray background (Boldt et al. 1978). If we attribute the X-ray background to a fairly uniform hot intergalacatic plasma, however, the amount of energy needed for heating could be prohibitive, even for quasars (Field and Perrenod 1977). At this stage, I think it is useful to pursue an alternate working hypothesis that the background arises from individual thermal sources and that such sources are not in general to be found at low redshift. Whether many quasars are sources such as this is an open question. Other possible objects

peculiar to an earlier epoch should be considered. For example, Bookbinder et al. (1979) looked into the possibility that young galaxies are the sources of the X-ray background and find that appropriate thermal X-ray emission might result from the galactic wind expected during the enhanced supernova activity early in the life of a galaxy. In general, we need to search for young sources with suitable spectra. If they are not to be found, we may be forced to learn something new about heating an intergalactic plasma. Or perhaps we are seeing a pronounced cosmological effect yet to be understood.

APPENDIX A

ANISOTROPY OF COSMIC X-RAY BACKGROUND

Deviations from isotropy for the extragalactic hard X-ray background could be crucial in our understanding of origins for this radiation. Using data from the A2 instrument on HEAO-1, Pravdo and Iwan (1979, private communication) find that large-scale galactic effects, although relatively weak in hard X-rays, do extend to fairly high galactic latitudes. Iwan is now attempting to model this unresolved galactic emission of hard X-rays, but the situation is not as simple as we would like.

Since the HEAO-1 observatory surveyed the sky with scan paths that follow great circles which always traverse the ecliptic poles, the most straightforward and reliable way to investigate possible weak global anisotropies of the cosmic background involves referring data to ecliptic coordinates. Figure 11 shows the geometry to be considered, expressed in ecliptic coordinates; latitude is β, longitude is λ. Great circle scan paths correspond to vertical lines in this representation. The ecliptic longitudes for the dual halfs of such great circles are given as λ and λ'. The locus of galactic equator crossings is shown by the solid curves. Some interesting directions indicated are as follows:

#1 is our velocity direction relative to distant galaxies, as discussed by Rubin et al. (1976); it's at longitude 49^{0}.

#2 is the direction of the Virgo cluster, at longitude 184^{o}.

#3 is at longitude 185^{o} and gives the direction for our velocity relative to the microwave background, as measured by Cheng et al. (1979).

#4 is at longitude 164^{o} and gives the direction for the microwave related velocity as measured by Smoot et al. (1977).

The preferred direction to be associated with the microwave background is clearly very close to the ecliptic equator, which makes it particularly well suited to studies carried out with the HEAO-1 observatory. To minimize galactic effects near this preferred direction, we isolate those data corresponding to the band within 24^{o} of the ecliptic plane; this band is outlined with dashed lines in Figure 12. Even so, galactic effects do become important when we consider longitudes close to where the galactic equator crosses the ecliptic plane (i.e. at longitudes 89^{o} and 269^{o}). Eliminating the contribution of resolved sources, we have determined the average surface brightness for the band within 24^{o} latitude of the ecliptic as a function of ecliptic longitude. Deviations from isotropy so obtained are represented in Figure 12.

The circle shown in Figure 12 represents isotropy. Percentage deviations up to about 1% are here plotted as a function of ecliptic longitude (λ). Each interval corresponds to a region of almost 10^{3} square degrees for which the surface brightness is determined to a statistical precision of $\sim$ 0.1 -0.2%. Recall that the galactic plane crosses the ecliptic equator at longi-

tudes 89^{0} and 269^{0}. To visually separate effects due to this, those deviations in isotropy expected to be influenced most by the proximity of the galactic plane are shown as dashed lines. In this representation, the preferred directions of interest are:

a) our velocity as determined by Smoot et al. (1977),

b) our velocity as determined by Cheng et al. (1979),

c) the longitude where the local supercluster (deVaucouleurs 1958) crosses the ecliptic equator.

Considering only the solid portion of this plot where galactic effects should be minimal, the left-right asymmetry is (0.50 ± 0.09)% and repeats for independent surveys separated by six months. If due to the Compton-Getting effect, our velocity relative to the proper frame of the X-ray background is consistent with that relative to the microwave background. However, if there is indeed a concentration of X-ray emitting sources in the local supercluster this might account for much of the observed asymmetry and is being investigated further. If due to our galaxy, we remain confused.

APPENDIX B

LUMINOSITY FUNCTION

We have approached the determination of the luminosity function from two points of view. McKee et al. (1980) have used the list of all Abell clusters through distance class 4 in the Leir - van den Bergh (1977) catalog to search the HEAO-1 A2 all-sky survey data for X-ray emitting clusters of galaxies and determine an X-ray luminosity function. For comparison, we started with the smaller sample of relatively bright X-ray sources detected at high galactic latitudes which were subsequently identified as clusters. For this collection of objects exceeding 1.5 R15 flux units for the A2 instrument (for definitions, see Marshall et al. 1979), it was found (Boldt et al. 1979b) that the luminosity function is consistent with that obtained by McKee et al. (1980) starting with a "complete" optically identified sample. Our sample satisfies the V/Vm test of Schmidt (1968,1977); viz: $\langle V/Vm \rangle = 0.44 \pm 0.06$. Although the 23 clusters involved are clearly within the present epoch (i.e. $z < 0.09$), only Virgo is associated with the local supercluster.

Considering high-latitude bright X-ray sources identified with isolated galaxies, we find that almost half are at redshifts less than $z = 0.01$. As pointed out by Piccinotti and Mushotzky (1980, private communication), the local supercluster could thereby introduce a significant bias in this sample. By lowering

the selection threshold to 1 R15 flux unit the relative proportion of more distant sources increases, and we obtain $\langle V/Vm \rangle = 0.49 \pm 0.05$. This larger sample was used for constructing the luminosity function presented in Figure 13, although the indicated normalization ($K \equiv NS^{1.5}$) is that obtained for S = 1.5 R15 units (i.e. K = 5.4). We exclude objects such as the quasar 3C273 at the high luminosity end and the normal galaxy M31 at the low end to obtain a sample that might properly be called active galaxies (see Table 3).

The luminosities used for Figure 13 are for the band 2 - 20 keV. For an energy index $\alpha = 0.7$, one R15 unit corresponds to 3.5×10^{-11} ergs cm^{-2} s^{-1} for 2 - 20 keV and 5.3×10^{-11} ergs cm^{-2} s^{-1} for 3 - 50 keV, the band used for our comparison with the X-ray background. The luminosity function is presented in integral form and is a power law over about three decades of luminosity. A power-law index of 1.5, as used by Pye and Warwick (1979), appears to be consistent with the data and is shown in Figure 13 for reference. A more critical evaluation of the luminosity function for active galaxies, based on HEAO-1 A2 data, is now underway by Piccinotti (1980, private communication).

TABLE 3: ISOLATED X-RAY EMITTING GALAXIES*
Used for this Study

M31	(B)	NGC526a	(A,B,C)	ESO 103-G35	(A)
M82	(B)	NGC0918	(B,C)	ESO 140-G43	(B,C)
Mkn142	(B)	NGC2910	(A)	ESO 141-G55	(A,B,C)
Mkn590	(B,C)	NGC2992	(A,B,C)	MCG 2-58-22	(A,B,C)
Mkn335	(B)	NGC3227	(C)	MCG 8-11-11	(A)
Mkn372	(B,C)	NGC3783	(A,B,C)		
Mkn421	(A)	NGC4151	(A,C)	PKS0548-322	(A,C)
Mkn464	(C)	NGC4593	(B)		
Mkn501	(A,B,C)	NGC5033	(C)	PKS2155-304	(A)
Mkn509	(A,B,C)	NGC5128	(A)	III Zw2	(B,C)
Mkn876	(B)	NGC5506	(C)	Fairall 9	(B,C)
3C111	(A)	NGC5548	(A,B,C)	4U 0241+62	(A)
3C120	(A,B,C)	NGC6814	(A)	H 0642+534**	(B)
3C273	(A)	NGC7172	(B,C)	4U 0945-30	(A)
3C371	(B)	NGC7213	(A,B,C)	2A1219+305	(A,B)
3C382	(A)	NGC7469	(A,B,C)	2A1347-300***	(A,C)
3C445	(B,C)	NGC7582	(A,C)	H1824+644	(B)

Sample A used for histogram of spectral indices (Fig. 7).

Sample B used for composite spectrum (see text, Fig. 9).

Sample C used for luminosity function (see Appendix B, Fig. 13).

* Includes BL Lac type objects and quasars.

** ANON 0636+53

*** IC4329A

REFERENCES

Bignami, G., Fichtel,C., Hartman, R. and Thompson,D. 1979, Ap. J. 232, 649.

Boldt, E., Marshall, F., Mushotzky,R., Holt, S.,Rothschild, R. and Serlemitsos, P. 1978, Bull. AAS 10, 501.

Boldt, E., Marshall, F., Mushotzky,R., Holt, S.,Rothschild,R., and Serlemitsos, P. 1979a, COSPAR X-ray Astronomy (edited by W. Baity and L. Peterson), Pergamon Press, Oxford, p. 443.

Boldt, E., Marshall, F., Mushotzky, R., Shafer, R., Stottlemyer, A., Holt, S., Serlemitsos, P., and McKee, J. 1979b, Bull. APS 24, 620.

Bookbinder, J., Cowie, L., Krolik, J., Ostriker, J., and Rees, M. 1979, preprint.

Cash, W. 1979, Bull. AAS 11, 723.

Cheng, E., Saulson, P., Wilkinson, D. and Corey, B. 1979, Ap. J. 232, L139.

deVaucouleurs, G. 1958, A.J. 63, 253.

Fichtel,C., Simpson, G., and Thompson,D. 1978, Ap. J. 222, 833.

Field, G., and Perrenod, S. 1977, Ap. J. 215, 717.

Giacconi, R., Bechtold, J., Branduardi,G., Forman, W., Henry, J., Jones, C., Kellogg, E., van der Laan, H., Liller, W., Marshall, H., Murray,S., Pye, J., Schreier, E., Sargent, W., Seward, F. and Tananbaum, H. 1979, Ap. J. 234, L1.

Kinzer, R., Johnson,W., and Kurfess, J. 1978,Ap. J. 222, 370.

Leir,A., and van den Bergh, S. 1977, Ap. J. (Suppl.) 3, 211.

Marshall, F., Boldt, E., Mushotzky,R., Pravdo, S., Rothschild, R., and Serlemitsos, P. 1979,Ap. J. (Suppl) 40, 657.

Marshall, F., Boldt, E., Holt, S., Miller, R., Mushotzky, R., Rose. L., Rothschild, R., and Serlemitsos, P. 1980, Ap. J. 235, 4.

Matteson, J., Gruber, D., Nolan, P., Peterson, L. and Kinzer, R. 1979, Bull. AAS 11, 653.

McKee, J., Mushotzky,R.,Boldt, E., Holt,S., Marshall,F., Pravdo, S. and Serlemitsos, P. 1980, Ap. J., submitted.

Murray, S. 1979, Bull. AAS 11, 642.

Mushotzky, R., Marshall, F., Boldt, E., Holt, S., and Serlemitsos, P. 1980, Ap. J. 235, 377.

Pye, J.P., and Warwick, R.S. 1979, Mon. Not. Roy. Astron. Soc. 187, 905.

Riegler, G., Agrawal, P., and Mushotzky, R. 1979, Ap. J. 233, L47.

Rothschild, R., Boldt, E., Holt, S., Serlemitsos, P., Garmire, G., Agrawal, P., Riegler, G., Bowyer, S., and Lampton, M. 1979, Space Science Instrumentation 4, 269.

Rubin, V., Ford, W., Thonnard, N., Roberts, M., and Gordon, J. 1976, A.J. 81, 687.

Schmidt, M. 1968, Ap. J. 151, 393.

Schmidt, M. 1977, in "Radio Astronomy and Cosmology - IAU Symp. No. 74", (ed. D. L. Jauncey) D. Reidel - Holland, 259.

Smoot, G., Gorenstein, M., and Muller, R. 1977, Phys. Rev. (Letters) 39, 898.

Trombka, J., Dyer, C., Evans, L., Bielefeld, M., Seltzer, S., and Metzger, A. 1978, Ap. J. 212, 925.

Wills, D. 1978, Physica Scripta 17, 333.

Worrall, D., Marshall, F., and Boldt, E. 1979, Nature 281, 127.

FIGURE CAPTIONS

Figure 1 - The surface brightness of the entire X-ray sky (in $3^0 \times 3^0$ pixels) as obtained with the combined $3^0 \times 3^0$ and $6^0 \times 3^0$ collimator sections of a high energy detector (HED-1 of HEAO-A2) over the band 2-60 keV. The map is presented in galactic coordinates. Intensity gradations are color-coded in the order black, blue and red (highest). Color print on request.

Figure 2 - The ratio (R) as a function of X-ray energy of the counts observed for the X-ray background to that predicted by convolving with the detector response function thermal bremsstrahlung incident spectra (characterized by kT = 25, 40, 60 keV). Different symbols are used to represent the first layer of the MED (medium energy detector) and both layers of HED 1 and HED 3. Statistical errors are shown when larger than the size of the symbols.

Figure 3 - Incident thermal spectrum (kT = 6.8 keV) for the Perseus cluster as inferred from data obtained with argon (MED) and xenon (HED) proportional counters of HEAO A2. Prominent lines in the 5-10 keV band correspond to Kα and Kβ transitions in iron ions having only K shell electrons.

Figure 4 - The X-ray spectrum for the BL Lac type object PKS 0548-322 as inferred from data obtained by a low energy detector (LED results from JPL indicated by crosses) and a medium energy detector (MED results from GSFC indicated by diamonds).

Figure 5 - The X-ray spectrum for Cen A as inferred from data obtained with a xenon proportional counter (HED), using the model of a power-law spectrum at the source absorbed by surrounding non-ionized matter exhibiting iron K fluorescence.

Figure 6 - The X-ray spectra for 5 Seyfert-1 type galaxies as inferred from data obtained with a xenon proportional counter (HED), using the model of a power-law spectrum at the source absorbed by surrounding non-ionized matter. Except for MCG8-11-11, all spectra shown are from pointed data. All are consistent with a power-law spectrum of photon number index $\approx$ 1.7; only NGC6814 requires significant absorption to fit the data.

Figure 7 - Histogram of energy spectral index (α) for X-ray emitting isolated galaxies listed in Table 3 as Sample A. For comparison, $(\Delta\alpha)_B$ gives the 90% confidence limits on α for the composite spectrum of Sample B (see Table 3).

Figure 8 - The ratio (R) as a function of X-ray energy of the counts observed for the X-ray background to that predicted by convolving with the detector response function power-law spectra (characterized by $\Gamma = 1.4$, $\Gamma = 1.7$). Different symbols are used to represent the first layer of the MED and both layers of HED 1 and HED 3. Statistical errors are shown when larger than the size of the symbols.

Figure 9 - Surface brightness of the extragalactic X-ray sky as a function of photon energy. The curve labelled "total flux" is the best-fit thermal spectrum (kT = 40 keV) for the background measured by Marshall et al. (1980). The power-law "A" represents the composite flux due to sources corresponding to those detected in the HEAO-2 deep exposures by Giacconi et al. (1979); see Table 2. The power-law "B" represents the composite flux from active galaxies for $z \leq 1$, based on the luminosity function determined with HEAO-1 A2 (Appendix B) and assuming no evolution. The dashed lines are extrapolations.

Figure 10 - Extragalactic gamma-ray background. Solid circles show data from the HEAO-1 A4 experiment (Matteson et al. 1979) and open circles summarize results obtained by Trombka et al. (1978). The dash-dot line is a power-law fit to data above 35 MeV (Fichtel et al. 1978). The dashed line starting at 100 keV is an extrapolation of power-law "B" of Figure 9. The solid curve gives the expected gamma-ray background as estimated from X-ray data at energies below 50 keV (see text).

Figure 11 - Special directions on the celestial sphere, expressed in ecliptic coordinates (Latitude is β, Longitude is λ). Great circle scan paths for HEAO-1 correspond to vertical lines. The ecliptic longitudes for the dual halfs of such great circles are designated λ and λ'. The locus of galactic equator crossings is shown by the solid curves. The galactic center is indicated as $\ell = 0$. The dashed lines outline the band within 24^{o} of the ecliptic plane used for evaluating anisotropies (see text). Special directions noted are #1) Longitude 49^{o} (Rubin et al. 1976), #2) Longitude 184^{o} (Virgo cluster), #3) Longitude 185^{o} (Cheng et al. 1979) and #4) Longitude 164^{o} (Smoot et al. 1977).

Figure 12 - Percentage deviations from isotropy (represented by the circle) for the average surface brightness near the ecliptic plane (β = $-24^{o} \rightarrow +24^{o}$) as a function of ecliptic longitude (λ). Data obtained with HED units in all-sky survey. Error bar shown is statistical. Special directions indicated are: a. Smoot et al. (1977), b. Cheng et al. (1979) and c. longitude where local supercluster crosses ecliptic equator. Surface brightness deviations for those longitudes close to the galactic equator (i.e. near ecliptic longitudes 89^{o} and 269^{o}) are indicated with dashed lines.

Figure 13 - The luminosity function for active galaxies is here presented as the number of sources, n(Mpc^{-3}), exceeding the indicated luminosity(L)

for the band 2-20 keV. Sm is the apparent luminosity threshold for this sample (i.e. Sm = 1 R15 unit), Vm is the volume in space accessible with such a threshold and evaluated separately for the luminosity of each source detected, N is the number of sources in the sample and K is the coefficient ($K = NS^{1.5}$) that normalizes the result to 4π coverage. H_o = 50 km s^{-1} Mpc^{-1} is used throughout.

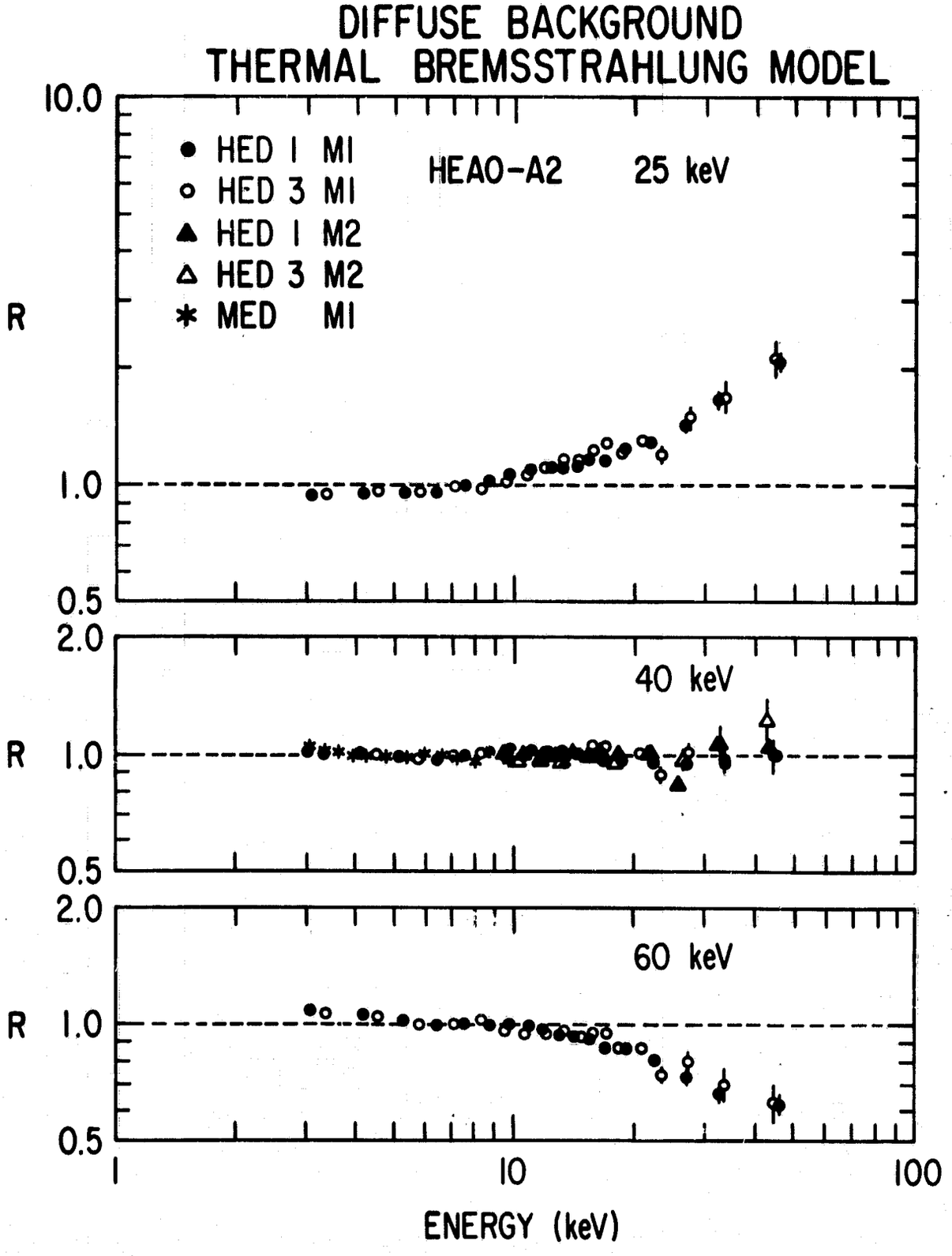
DIFFUSE BACKGROUND
THERMAL BREMSSTRAHLUNG MODEL
HED 1 M1
HED 3 M1
HED 1 M2
HED 3 M2
MED M1
HEAO-A2 25 keV
40 keV
60 keV
R
10.0
2.0
1.0
0.5
1
10
100
ENERGY (keV)

Figure 2

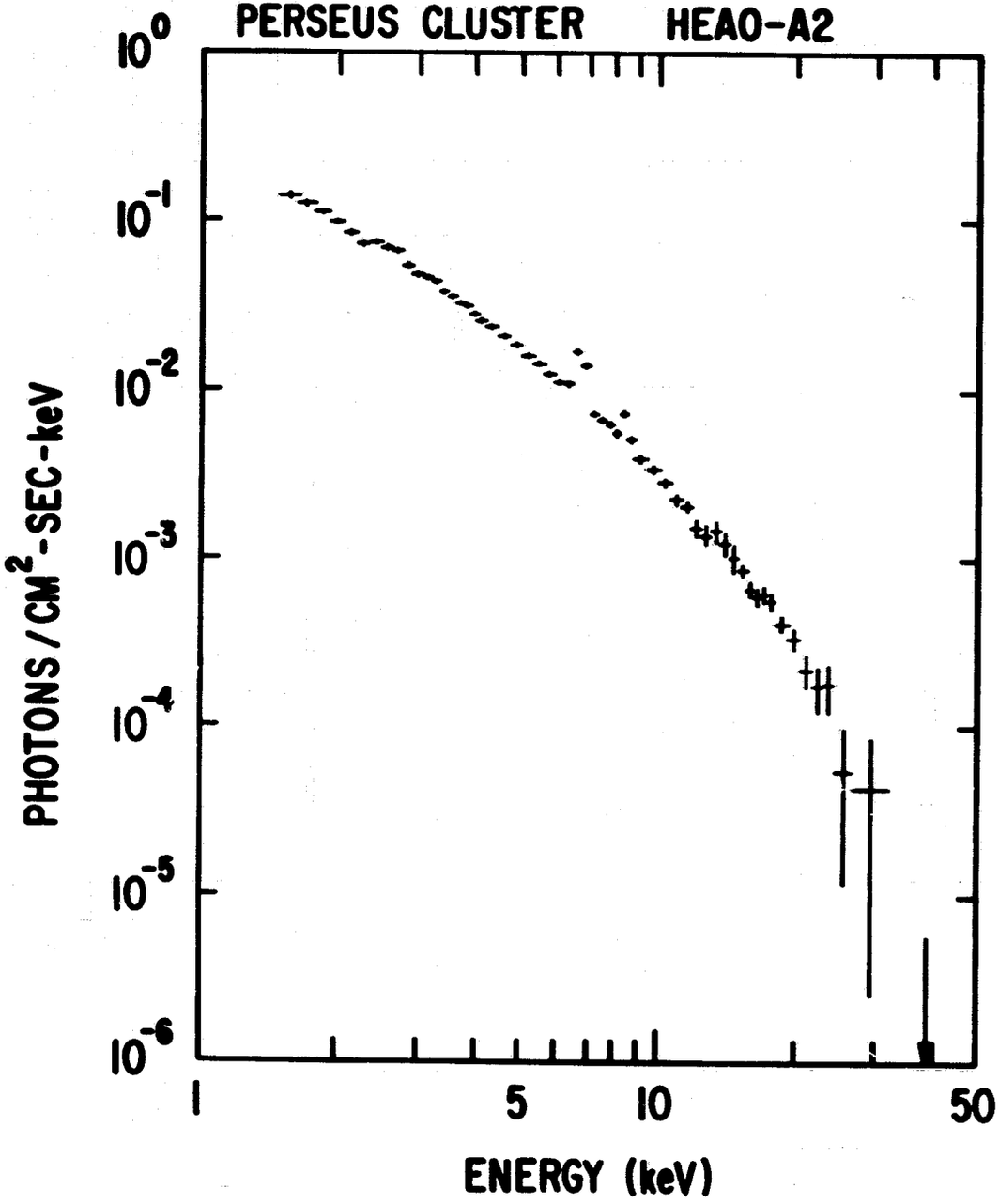
PERSEUS CLUSTER HEAO-A2
PHOTONS/CM^2-SEC-keV
10^0
10^{-1}
10^{-2}
10^{-3}
10^{-4}
10^{-5}
10^{-6}
1
5
10
50
ENERGY (keV)

Figure 3

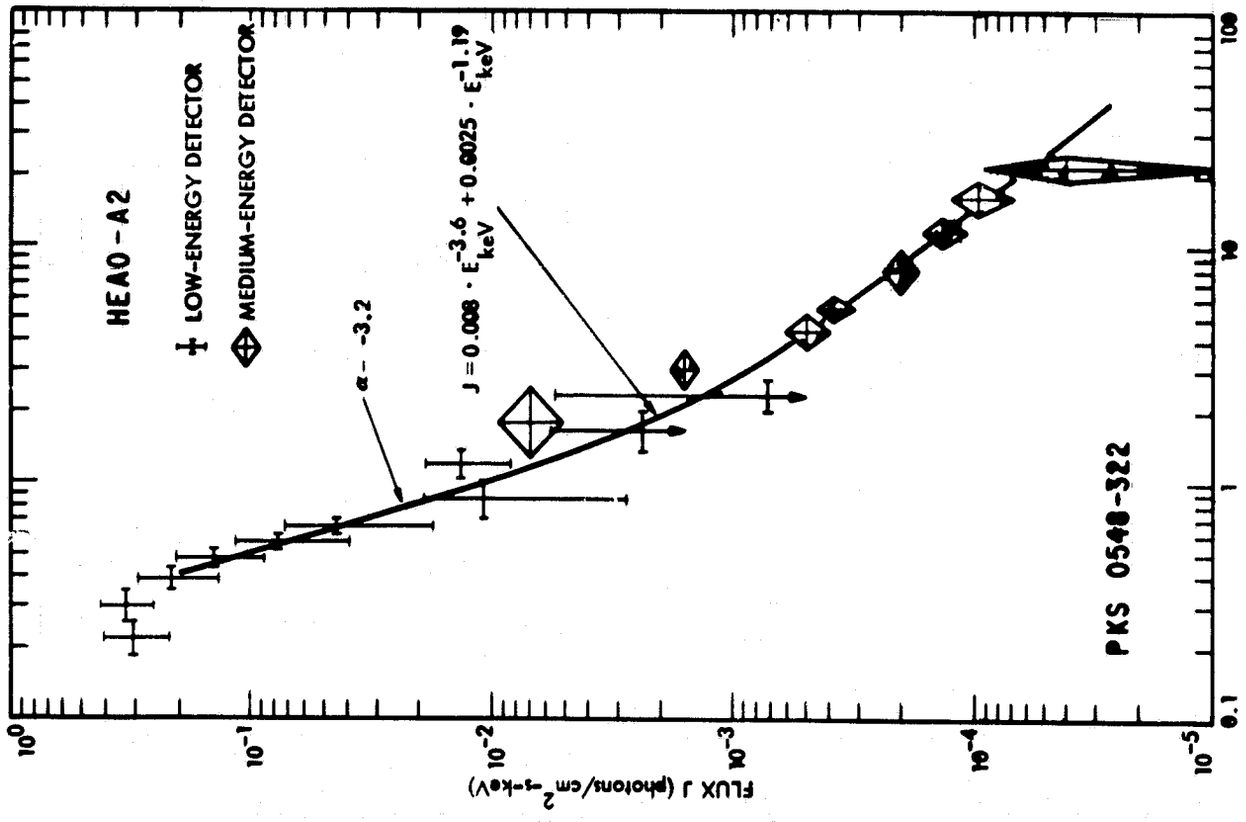
HEAO - A2
LOW-ENERGY DETECTOR
MEDIUM-ENERGY DETECTOR
α = -3.2
J = 0.008 · E_keV^-3.6 + 0.0025 · E_keV^-1.19
PKS 0548-322
FLUX J (photons/cm²-s-keV)
ENERGY (keV)
10^0
10^-1
10^-2
10^-3
10^-4
10^-5
0.1
1
10
100

Figure 4

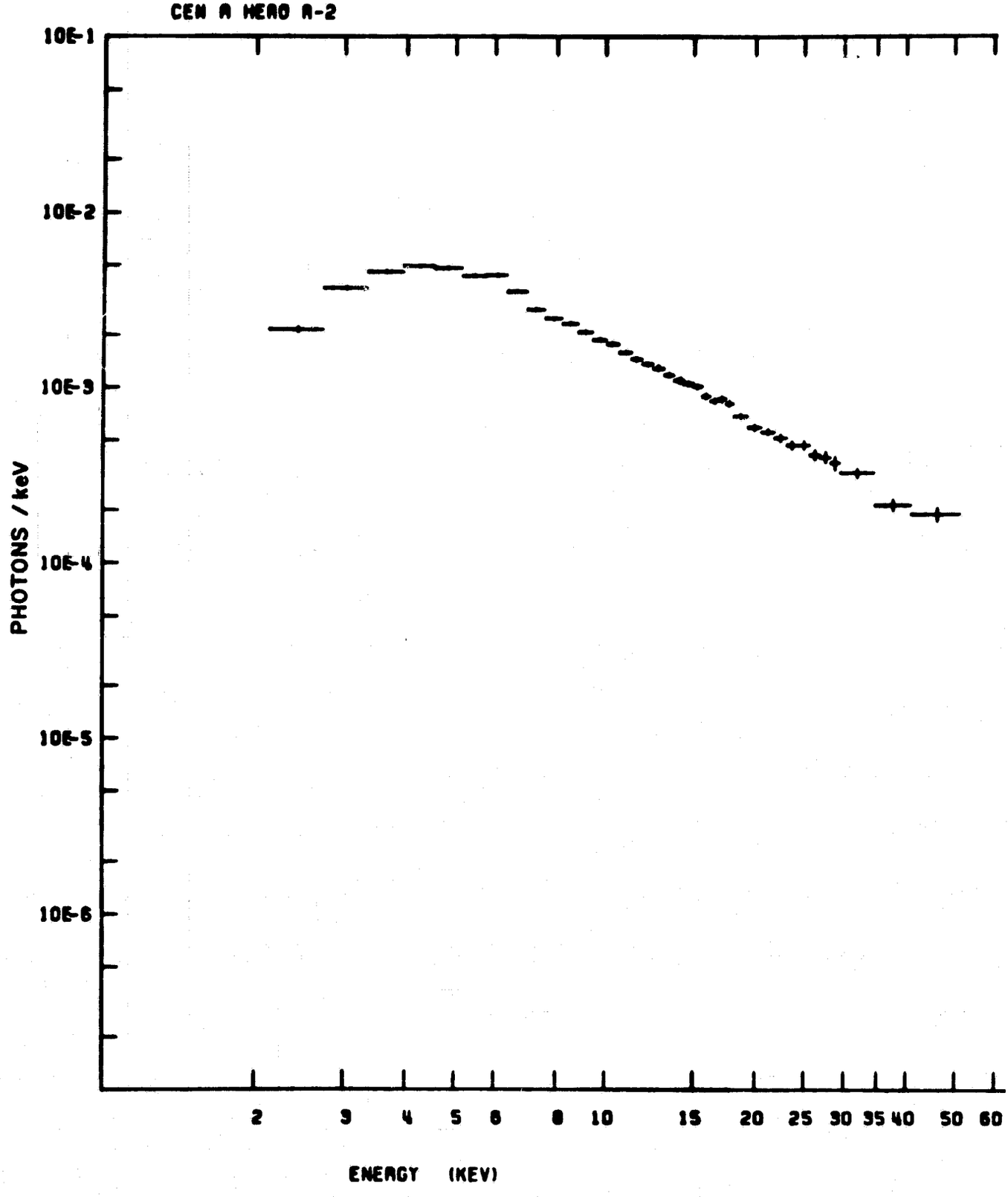
CEN A HEAO A-2
10E-1
10E-2
10E-3
10E-4
10E-5
10E-6
PHOTONS / keV
2
3
4
5
6
8
10
15
20
25
30
35
40
50
60
ENERGY (KEV)

Figure 5

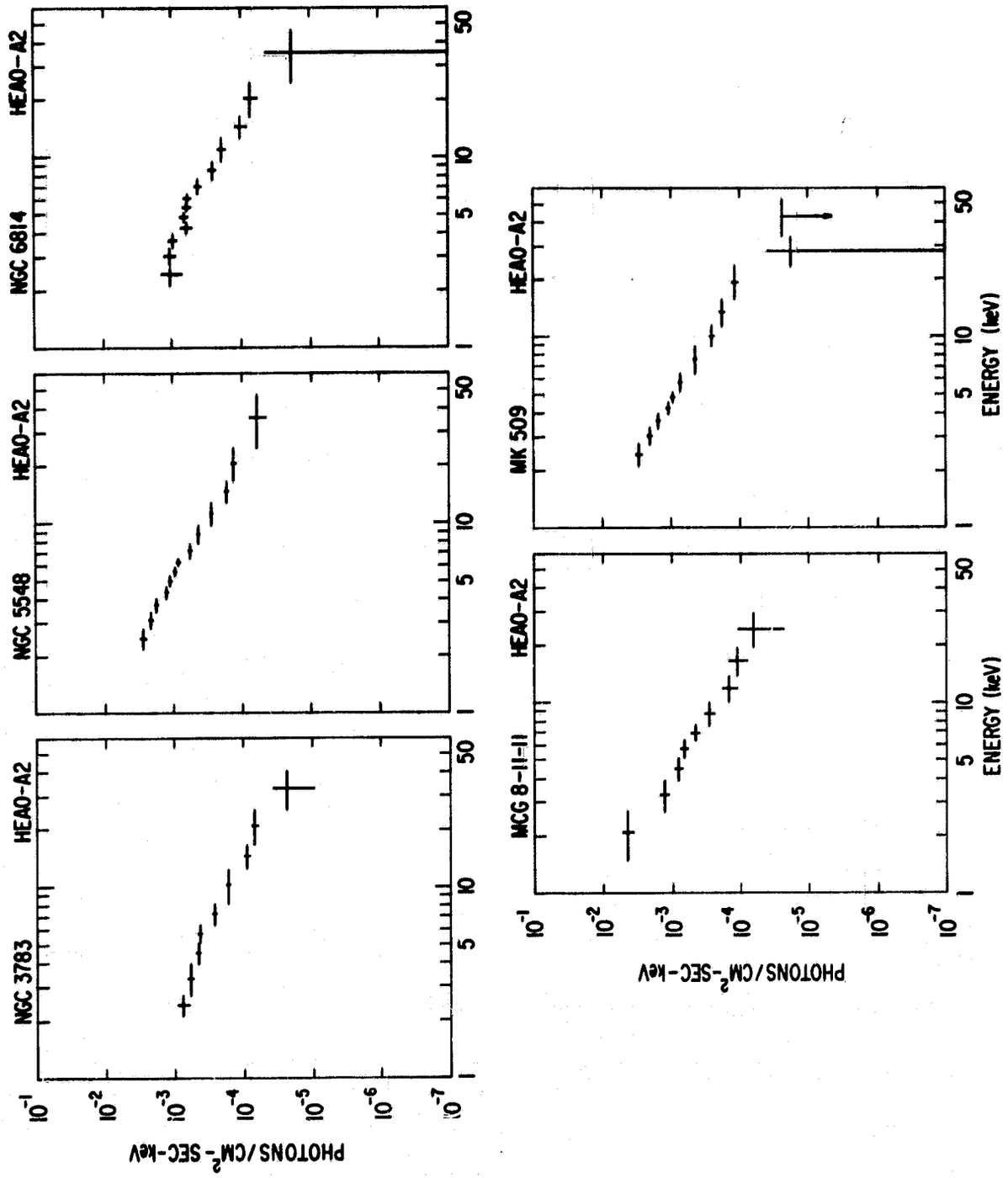
NGC 6814
HEAO-A2
NGC 5548
HEAO-A2
NGC 3783
HEAO-A2
MK 509
HEAO-A2
MCG 8-11-11
HEAO-A2
ENERGY (keV)
ENERGY (keV)
PHOTONS/CM²-SEC-keV
PHOTONS/CM²-SEC-keV

Figure 6

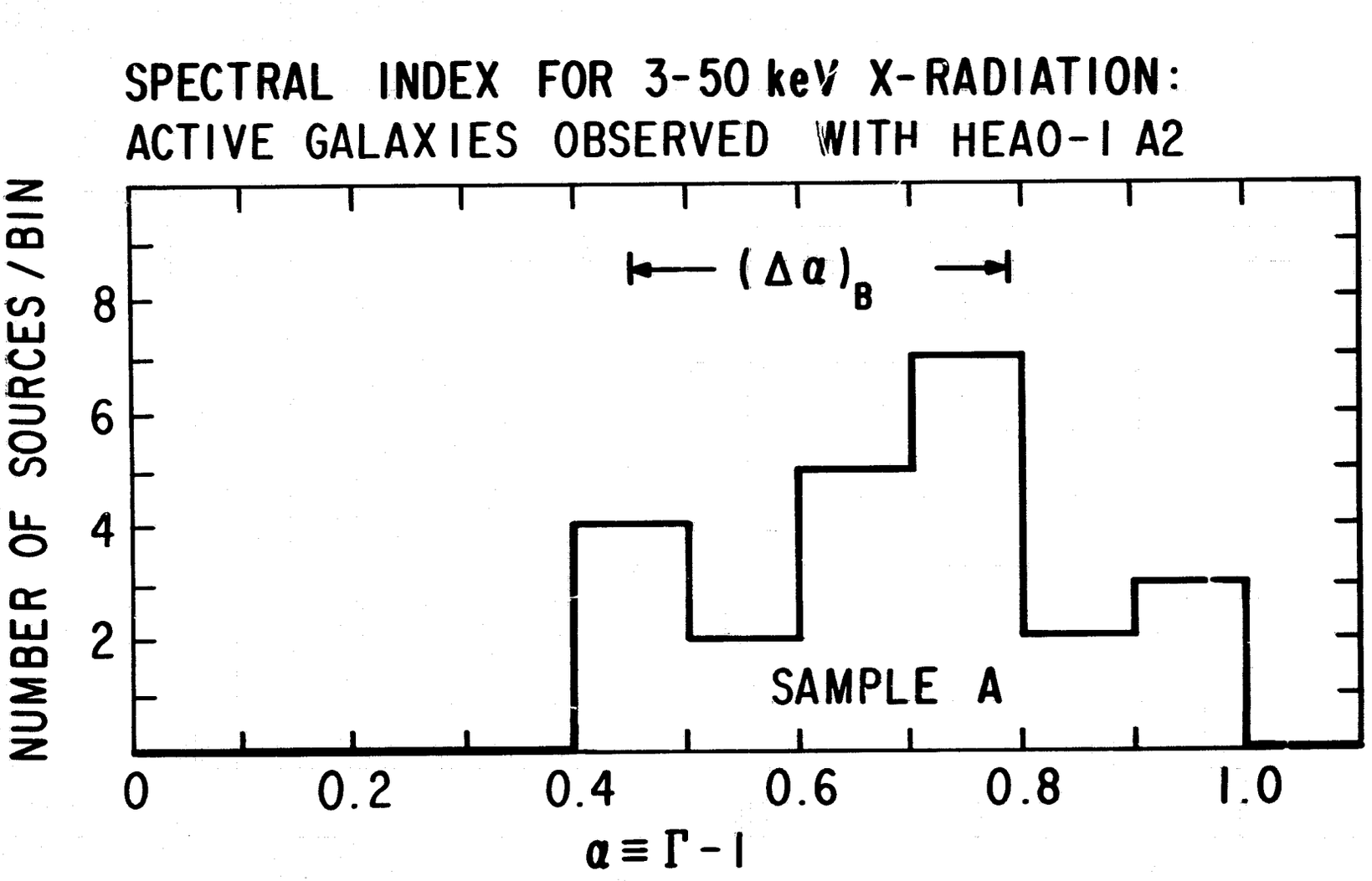
SPECTRAL INDEX FOR 3-50 keV X-RADIATION:
ACTIVE GALAXIES OBSERVED WITH HEAO-1 A2
NUMBER OF SOURCES / BIN
(Δα)B
SAMPLE A
0
0.2
0.4
0.6
0.8
1.0
2
4
6
8
α ≡ Γ - 1

Figure 7

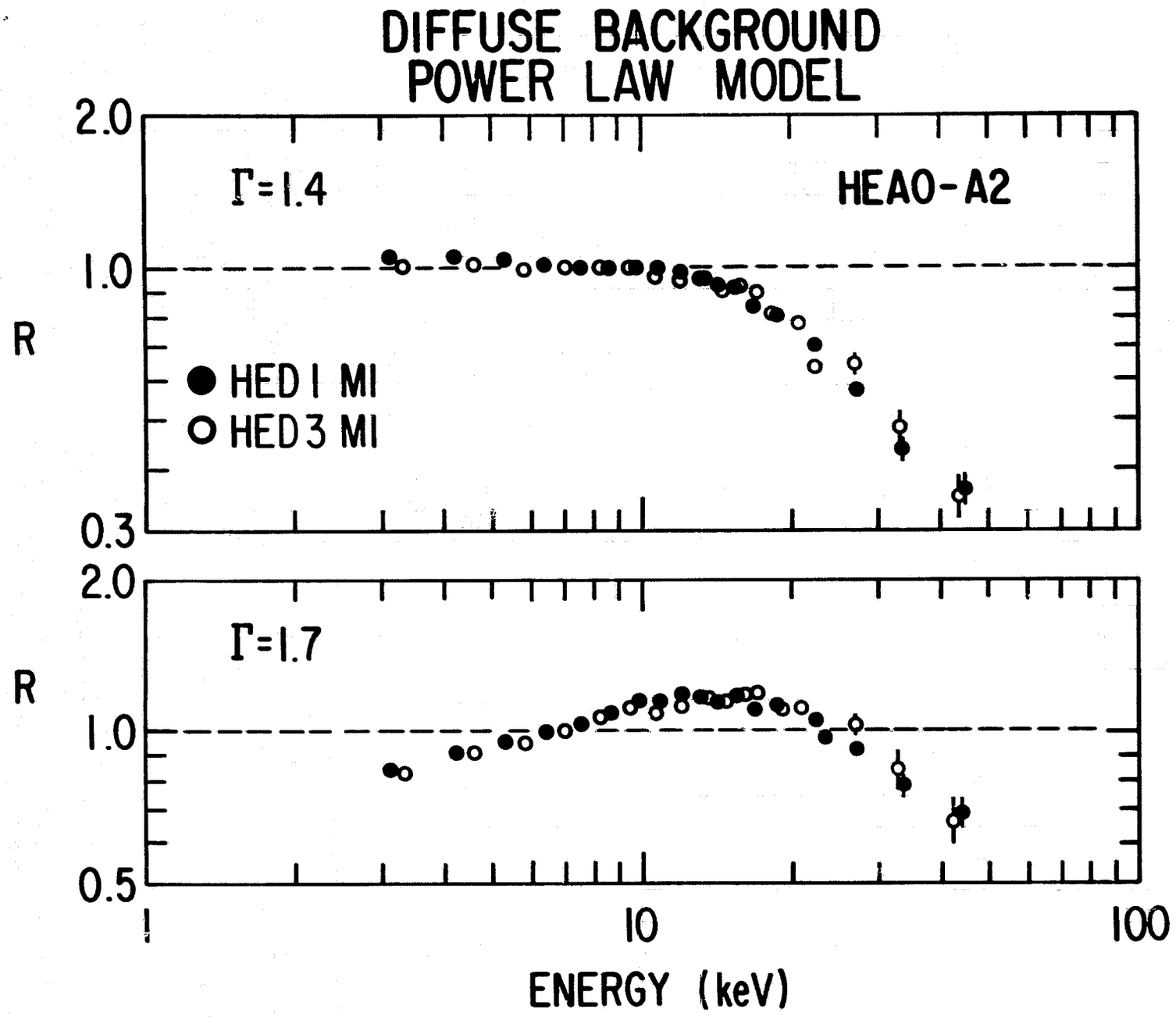
DIFFUSE BACKGROUND
POWER LAW MODEL
Γ=1.4
HEAO-A2
HED 1 MI
HED 3 MI
Γ=1.7
R
2.0
1.0
0.3
0.5
1
10
100
ENERGY (keV)

Figure 8

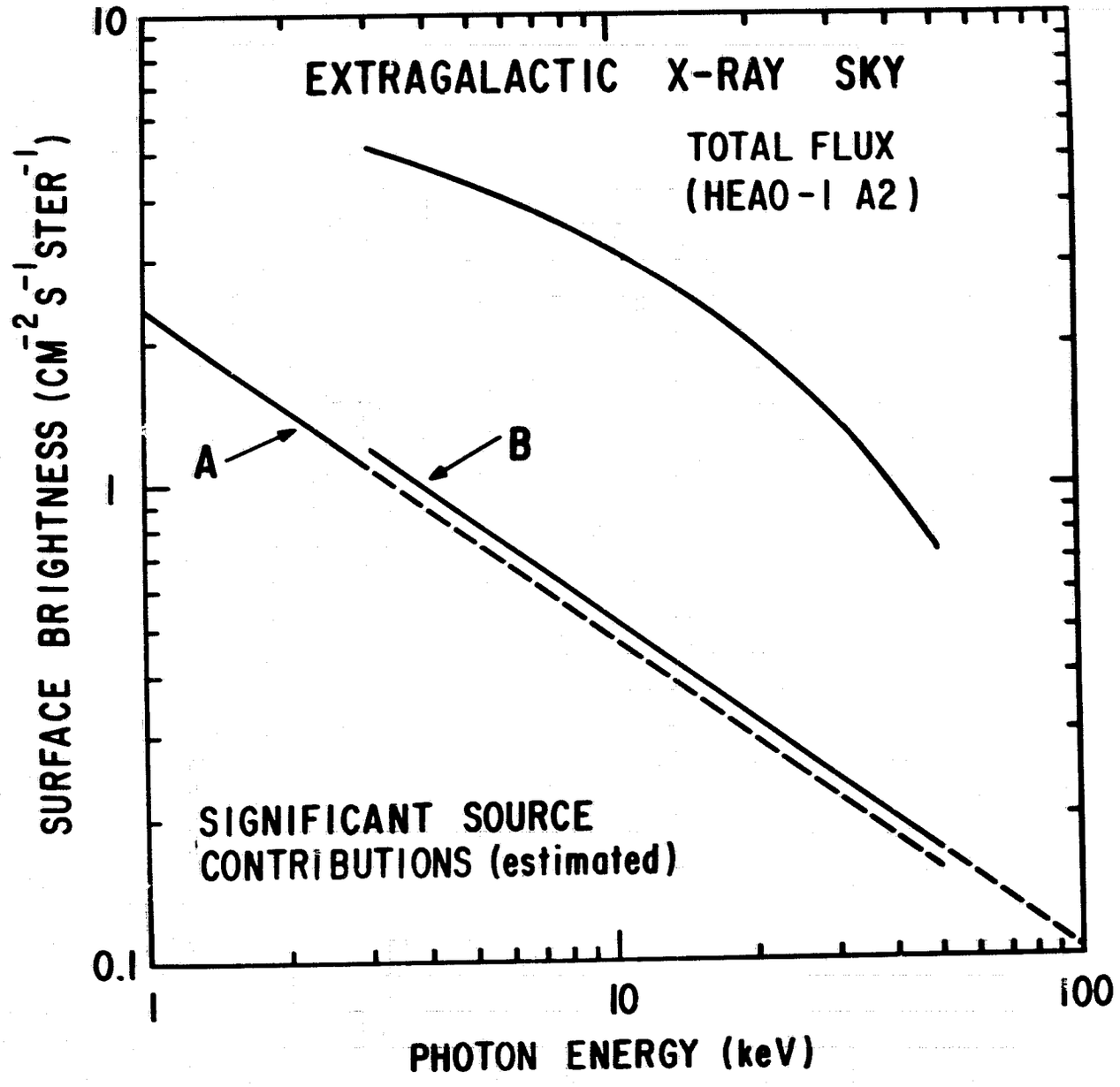
EXTRAGALACTIC X-RAY SKY
TOTAL FLUX
(HEAO-1 A2)
A
B
SIGNIFICANT SOURCE
CONTRIBUTIONS (estimated)
SURFACE BRIGHTNESS (CM^{-2}S^{-1}STER^{-1})
10
1
0.1
1
10
100
PHOTON ENERGY (keV)

Figure 9

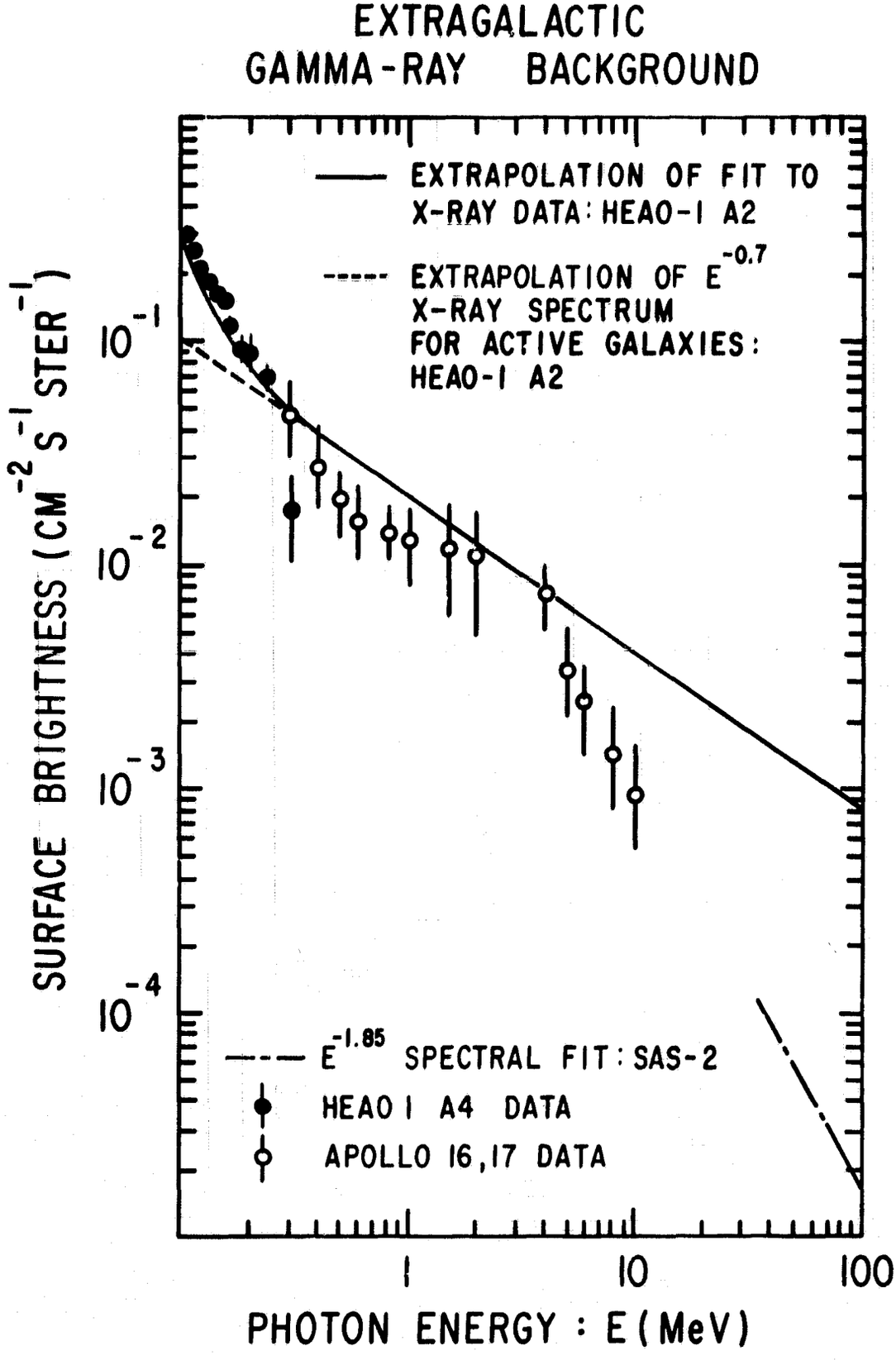
EXTRAGALACTIC
GAMMA-RAY BACKGROUND
EXTRAPOLATION OF FIT TO
X-RAY DATA: HEAO-1 A2
EXTRAPOLATION OF E^-0.7
X-RAY SPECTRUM
FOR ACTIVE GALAXIES:
HEAO-1 A2
SURFACE BRIGHTNESS (CM^-2 S^-1 STER^-1)
10^-1
10^-2
10^-3
10^-4
E^-1.85 SPECTRAL FIT: SAS-2
HEAO 1 A4 DATA
APOLLO 16,17 DATA
1
10
100
PHOTON ENERGY : E (MeV)

Figure 10

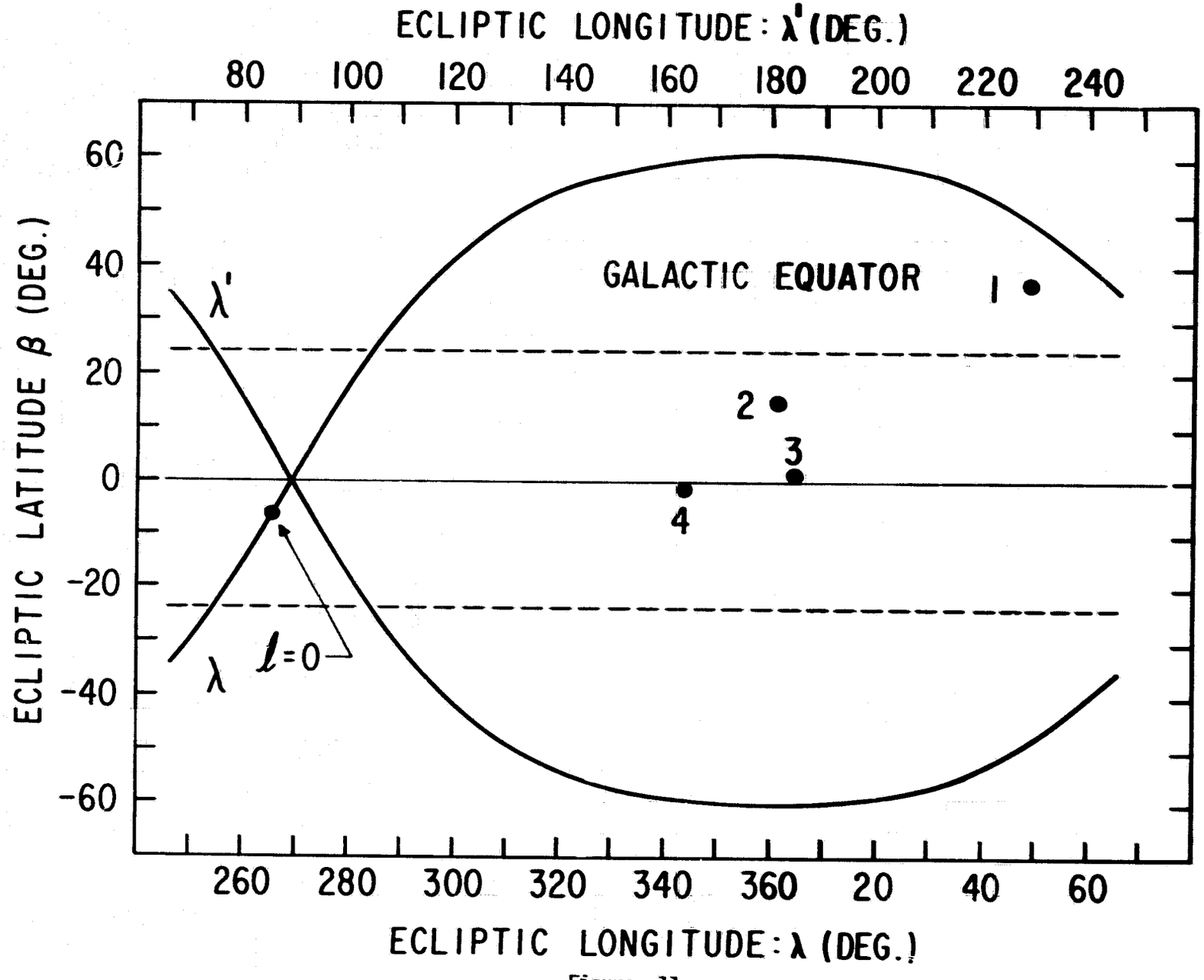
ECLIPTIC LONGITUDE: λ' (DEG.)
80
100
120
140
160
180
200
220
240
60
40
20
0
-20
-40
-60
ECLIPTIC LATITUDE β (DEG.)
GALACTIC EQUATOR
λ'
λ
ℓ=0
1
2
3
4
260
280
300
320
340
360
20
40
60
ECLIPTIC LONGITUDE: λ (DEG.)

Figure 11

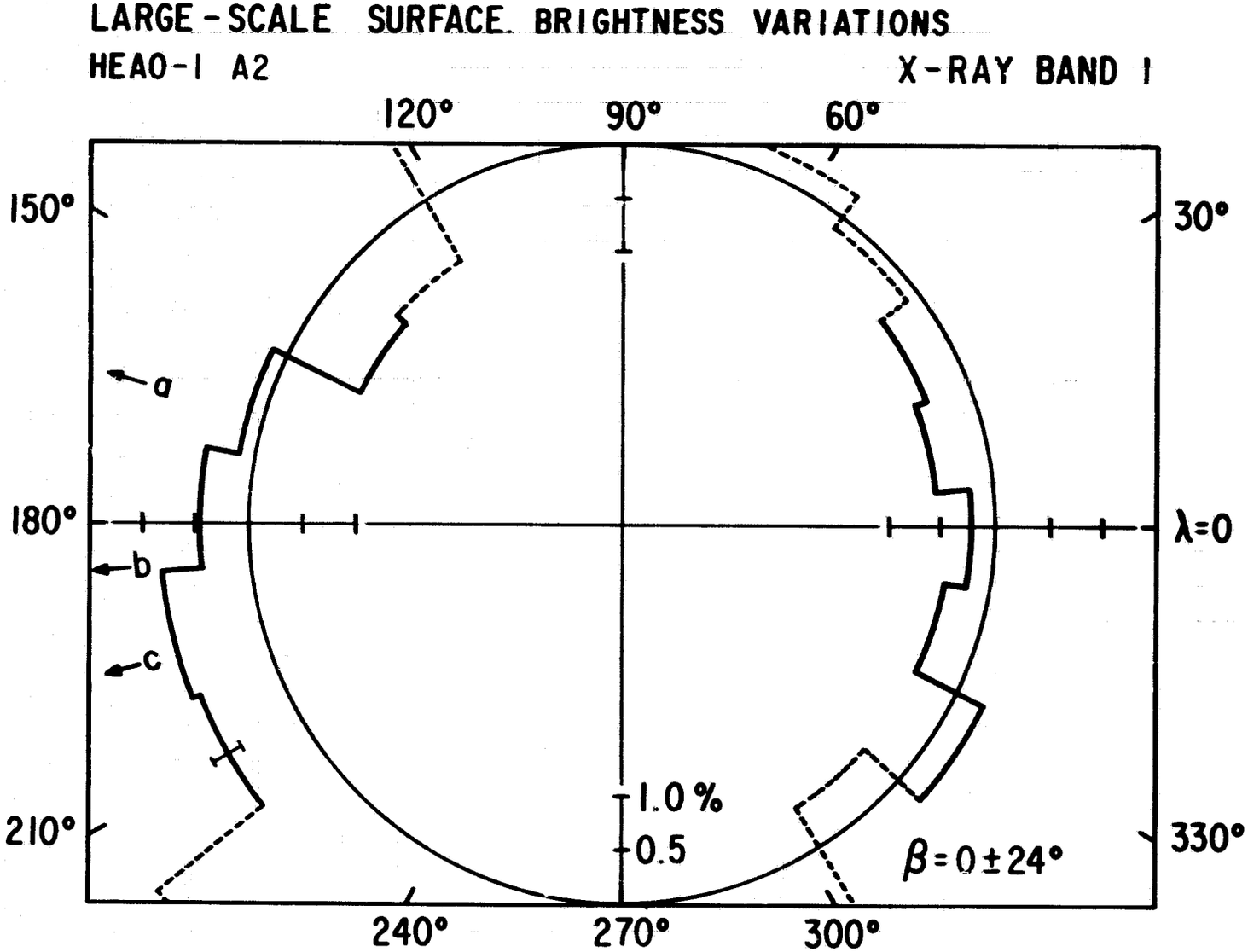
LARGE-SCALE SURFACE BRIGHTNESS VARIATIONS
HEAO-1 A2
X-RAY BAND 1
120°
90°
60°
150°
30°
a
180°
λ=0
b
c
210°
330°
1.0 %
0.5
β=0±24°
240°
270°
300°
PERCENT DEVIATIONS FROM AVERAGE
VERSUS ECLIPTIC LONGITUDE (λ)

Figure 12

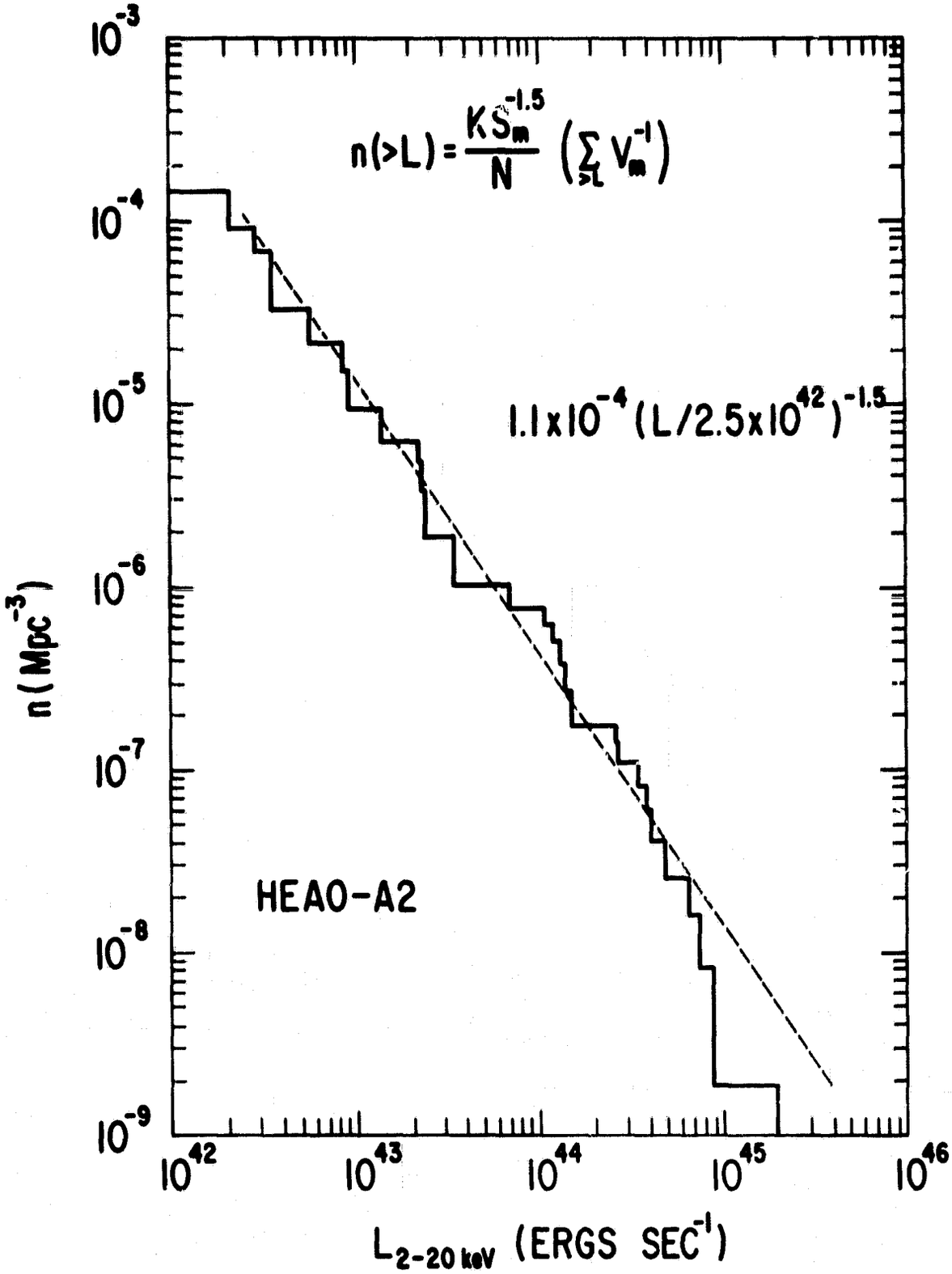
LUMINOSITY FUNCTION FOR ACTIVE GALAXIES
$n(>L) = \frac{K S_m^{-1.5}}{N} \left(\sum_{>L} V_m^{-1}\right)$
$1.1 \times 10^{-4} (L/2.5 \times 10^{42})^{-1.5}$
HEAO-A2
$n\,(Mpc^{-3})$
10^{-3}
10^{-4}
10^{-5}
10^{-6}
10^{-7}
10^{-8}
10^{-9}
10^{42}
10^{43}
10^{44}
10^{45}
10^{46}
$L_{2\text{-}20\,keV}$ (ERGS SEC^{-1})

Figure 13

BIBLIOGRAPHIC DATA SHEET

1. Report No.	2. Government Accession No.	3. Recipient's Catalog No.
TM 80659		

4. Title and Subtitle	5. Report Date
The Cosmic X-Ray Background	March 1980
	6. Performing Organization Code: 661
7. Author(s): Erihu Boldt	8. Performing Organization Report No.
9. Performing Organization Name and Address: Cosmic Radiations Branch, Laboratory for High Energy Astrophysics, NASA/Goddard Space Flight Center, Greenbelt, MD 20771	10. Work Unit No.
	11. Contract or Grant No.
	13. Type of Report and Period Covered
12. Sponsoring Agency Name and Address	14. Sponsoring Agency Code

15. Supplementary Notes

Invited Lecture at the 155th Meeting, American Astronomical Society, San Francisco, California, January 15, 1980

16. Abstract

The cosmic X-ray experiment carried out with the A2 Instrument on HEAO-1 was especially developed to make systematics-free measurements of the extragalactic X-ray sky and has yielded the broadband spectral characteristics for two extreme aspects of this radiation. For the apparently isotropic radiation of cosmological origin that dominates the extragalactic X-ray flux (> 3 keV), the spectrum over the energy band of maximum intensity is remarkably well described by a thermal model with a temperature of a half-billion degrees (i.e. kT $\approx$ 40 keV). At the other extreme, broadband observations of individual extragalactic X-ray sources with HEAO-1 are restricted to objects within the present epoch. These X-ray sources include a large sample of active galaxies studied in some detail over a broad bandwidth for the first time. While the non-thermal hard spectral components associated with unevolved X-ray emitting active galaxies could account for most of the gamma-ray background, the contribution of such sources to the X-ray background must be relatively small. In contrast, the "deep-space" sources detected in soft X-rays with the Einstein Observatory (HEAO-2) telescope probably represent a major portion of the extragalactic soft X-ray (< 3 keV) background, the characteristics of which are not yet firmly established.

17. Key Words (Selected by Author(s))	18. Distribution Statement

19. Security Classif. (of this report)	20. Security Classif. (of this page)	21. No. of Pages	22. Price*
U	U	40	

*For sale by the National Technical Information Service, Springfield, Virginia 22151.